

# Properties of the Recombinant Ferredoxin-Dependent Glutamate Synthase of *Synechocystis* PCC6803. Comparison with the *Azospirillum brasilense* NADPH-Dependent Enzyme and Its Isolated $\alpha$ Subunit<sup>†</sup>

Sergio Ravasio,<sup>‡</sup> Laura Dossena,<sup>‡</sup> Eugenio Martin-Figueroa,<sup>§</sup> Francisco J. Florencio,<sup>§</sup> Andrea Mattevi,<sup>||</sup> Paola Morandi,<sup>‡</sup> Bruno Curti,<sup>‡</sup> and Maria A. Vanoni<sup>\*,⊥</sup>

Dipartimento di Fisiologia e Biochimica Generali, Università di Milano, Milano, Italy, Instituto de Bioquímica Vegetal y Fotosíntesis, Centro de Investigaciones Científicas Isla de la Cartuja, Universidad de Sevilla-CSIC, Seville, Spain, Dipartimento di Genetica e Microbiologia, Università di Pavia, Pavia, Italy, and Dipartimento di Scienze Chimiche, Fisiche e Matematiche, Università dell'Insubria, Como, Italy

Received January 25, 2002; Revised Manuscript Received April 24, 2002

**ABSTRACT:** The properties of the recombinant ferredoxin-dependent glutamate synthase of *Synechocystis* PCC6803 were determined by means of kinetic and spectroscopic approaches in comparison to those exhibited by the bacterial NADPH-dependent enzyme form. The ferredoxin-dependent enzyme was found to be similar to the bacterial glutamate synthase  $\alpha$  subunit with respect to cofactor content (one FMN cofactor and one [3Fe-4S] cluster per enzyme subunit), overall absorbance properties, and reactivity of the FMN N(5) position with sulfite, as expected from the similar primary structure of ferredoxin-dependent glutamate synthase and of the bacterial NADPH-dependent glutamate synthase  $\alpha$  subunit. The ferredoxin- and NADPH-dependent enzymes were found to differ with respect to the apparent midpoint potential values of the FMN cofactor and of the [3Fe-4S] cluster, which are less negative in the ferredoxin-dependent enzyme form. This feature is, at least in part, responsible for the efficient oxidation of L-glutamate catalyzed by this enzyme form, but not by the bacterial NADPH-dependent counterpart. At variance with earlier reports on ferredoxin-dependent glutamate synthase, in the *Synechocystis* enzyme the [3Fe-4S] cluster is not equipotential with the flavin cofactor. The present studies also demonstrated that binding of reduced ferredoxin to ferredoxin-dependent glutamate synthase is essential in order to activate reaction steps such as glutamine binding, hydrolysis, or ammonia transfer from the glutamine amidotransferase site to the glutamate synthase site of the enzyme. Thus, ferredoxin-dependent glutamate synthase seems to control and coordinate catalytic activities taking place at its subsites by regulating the reactions of the glutamine amidotransferase site. Association with reduced ferredoxin appears to be necessary, but not sufficient, to trigger the required activating conformational changes.

Glutamate synthase (GltS)<sup>1</sup> forms with glutamine synthetase the main ammonia assimilation pathway in bacteria, microorganisms, and plants by catalyzing the reductive transfer of the glutamine amide group (L-Gln) to the C(2) carbon of 2-oxoglutarate (2-OG) with net production of L-glutamate (L-Glu). Bacteria contain an NADPH-dependent form of the enzyme (NADPH-GltS), which is composed of two dissimilar subunits ( $\alpha$  subunit, 162 kDa, and  $\beta$  subunit, 52.3 kDa, for the *Azospirillum brasilense* enzyme; 1). The

two subunits form the catalytically active  $\alpha\beta$  holoenzyme, which contains 1 FAD, 1 FMN, and three different Fe-S centers (Scheme 1). The  $\beta$  subunit functions as a FAD-dependent NADPH oxidoreductase, which serves to transfer reducing equivalents to the site of glutamate synthesis on the  $\alpha$  subunit through the enzyme [3Fe-4S] cluster (on the  $\alpha$  subunit) and at least one of its [4Fe-4S] centers (1, 2; Scheme 1). The  $\alpha$  subunit, whose three-dimensional structure has been recently determined (3), contains the GltS L-glutamine amidotransferase (GAT) site where L-Gln binds and is hydrolyzed to yield L-Glu and ammonia. The latter is transferred through the intramolecular ammonia tunnel (3) to the glutamate synthase site where 2-OG binds, is converted

<sup>†</sup> This research was carried out with funds from Consiglio Nazionale delle Ricerche, Target Project on Biotechnology (1999–2001), Ministero dell'Università e della Ricerca Scientifica e Tecnologica MURST-40%/FIRST, PRIN99 and 01, Rome, Italy, and Ministerio de Ciencia y Tecnología BCM 2001-2635, Spain. Personnel exchange between the Milano and Seville laboratories was supported by a grant within the Italy–Spain Integrated Action Program, HI1998-0244.

\* To whom correspondence should be addressed c/o Dipartimento di Fisiologia e Biochimica Generali, Via Celoria 26, 20131 Milano, Italy. Phone: +390250314901. Fax: +390250314895. E-mail: mav@mailserver.unimi.it.

<sup>‡</sup> Università di Milano.

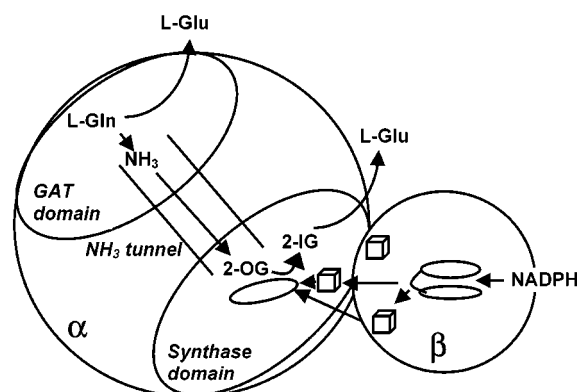
<sup>§</sup> Universidad de Sevilla-CSIC.

<sup>||</sup> Università di Pavia.

<sup>⊥</sup> Università dell'Insubria.

<sup>1</sup> Abbreviations: GltS, glutamate synthase; NAD(P)H-GltS, NAD(P)H-dependent GltS; Fd-GltS, ferredoxin-dependent GltS; Ab-GltS, *Azospirillum brasilense* GltS; 2-OG, 2-oxoglutarate; Fd, ferredoxin; GAT, L-glutamine-dependent amidotransferase; INT, iodonitrotetrazolium [2-(4-iodophenyl)-3-(4-nitrophenyl)-5-phenyltetrazolium chloride]; FPLC, fast protein liquid chromatography; TCA, trichloroacetic acid; L-DON, 6-diazo-5-oxo-L-norleucine;  $K_d$ , dissociation constant;  $K_{eq}$ , equilibrium constant;  $v$ , initial velocity;  $V$ , maximum velocity or apparent maximum velocity, depending on context;  $K$ , (apparent) Michaelis constant; FMN-ox, -sq, or -hq, oxidized, semiquinone, or hydroquinone forms of FMN.

Scheme 1: Schematic Drawing of the Location of Cofactors and Catalytic Subsites in *A. brasilense* Glutamate Synthase<sup>a</sup>



<sup>a</sup> The FAD cofactor and the [4Fe-4S] clusters of the  $\beta$  subunit are indicated as the two linked ovals and the two cubes, respectively. The FMN cofactor and the [3Fe-4S] cluster of the  $\alpha$  subunit are indicated by an oval and a cube, respectively. The arrows connecting FAD and FMN through two of the three [Fe-S] indicate the electron-transfer pathway between the flavins as deduced from the distribution of the  $E_m$  values of the centers (2).

to the iminoglutarate (2-IG) intermediate, and reduced to L-Glu by receiving reducing equivalents from the reduced FMN cofactor at this site (Schemes 1 and 2).

Plants produce two GltS forms: (i) a ferredoxin-dependent species (Fd-GltS) similar in size, primary structure, and cofactor content to the  $\alpha$  subunit of bacterial NADPH-GltS and (ii) an NADH-dependent GltS (NADH-GltS), which appears to derive from the fusion of polypeptides corresponding to the bacterial NAD(P)H-GltS  $\alpha$  and  $\beta$  subunits. The latter enzyme form has been poorly characterized biochemically. On the basis of sequence similarities, it is most likely very similar to NADPH-GltS with respect to cofactor content and catalytic properties. Open reading frames encoding NADH-GltS have been found in several lower eukaryotes such as *Saccharomyces cerevisiae*, *Caenorhabditis elegans*, *Plasmodium falciparum*, and *Drosophila melanogaster*, and the enzyme has been purified from yeast, *Medicago sativa*, and *Bombyx mori* (as reviewed in ref 1).

*Synechocystis* sp. strain PCC6803, a cyanobacterium whose complete genome sequence has been recently determined (CyanoBase, <http://www.kazusa.or.jp/cyano/>), is unique among photosynthetic organisms in which GltS activities have been found (4). It contains a plant-type Fd-GltS (165476 Da,<sup>2</sup> encoded by the *glsF* gene, CyanoBase accession code sl11499) along with a pyridine nucleotide-dependent GltS. The latter enzyme form is composed by two dissimilar subunits of 164476 and 54013 Da,<sup>2</sup> encoded by *gltB* and *gltD* genes, respectively (CyanoBase accession codes sl11502 and sl11027), similar in sequence to those of bacterial NADPH-GltS. However, the *Synechocystis* pyridine nucleotide-dependent GltS is reported to be NADH-dependent, as in the case of single subunit eukaryotic pyridine nucleotide-dependent GltS (4). Finally, at variance with other bacterial GltS the *gltD* and *gltB* genes encoding the small and large

subunits, respectively, are not adjacent on the *Synechocystis* chromosome.

The cyanobacterial Fd-dependent GltS form exhibits a high degree of sequence similarity with other plant Fd-GltS, with the  $\alpha$  subunit of NADPH-GltS and with the N-terminal three-fourths of eukaryotic NADH-GltS (1, 4). Interestingly, conserved residues in all of these enzymes map in regions of GltS  $\alpha$  subunit structure, which are crucial for formation of the catalytic subsites and the enzyme ammonia tunnel (1, 3). The single polypeptide chain of Fd-GltS contains 1 FMN and 1 [3Fe-4S] cluster and catalyzes glutamate synthesis using glutamine, 2-oxoglutarate, and reducing equivalents provided through reversible association with reduced ferredoxin (4). Thus, ferredoxin functionally substitutes the bacterial NADPH-GltS  $\beta$  subunit and the corresponding part of the eukaryotic NADH-GltS. *Synechocystis* Fd-GltS has been recently overproduced in *Escherichia coli* cells (4). A method for the obtainment of homogeneous preparations of enzyme was developed, and the recombinant *Synechocystis* Fd-GltS was shown to exhibit overall properties similar to those reported for Fd-GltS prepared from other sources (4, 5).

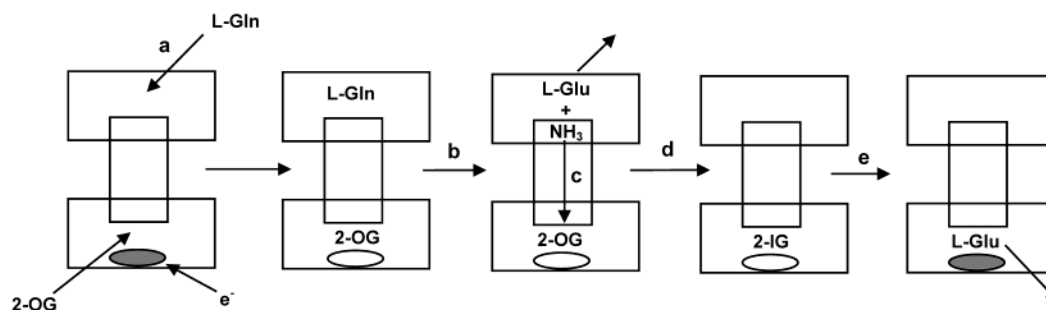
In this work we extended the characterization of recombinant *Synechocystis* Fd-GltS by means of kinetic and spectroscopic approaches. The results are discussed in comparison with the known properties of *A. brasilense* NADPH-GltS (Ab-GltS) for which a relatively large body of information is available with respect to the spectroscopic and catalytic properties of the holoenzyme (1, 2, 6) and of its isolated  $\alpha$  (2, 7) and  $\beta$  (1, 8) subunits and, recently, the three-dimensional structure of the  $\alpha$  subunit (3).

## EXPERIMENTAL PROCEDURES

**Enzymes.** Recombinant *Synechocystis* PCC6803 Fd-GltS, *A. brasilense* GltS holoenzyme, and its  $\alpha$  subunit were overproduced in *E. coli* cells and purified as described previously (refs 4, 6, and 7, respectively).

*Synechocystis* ferredoxin (Fd) was also overproduced in *E. coli* cells (9). It was purified to homogeneity by coupling modifications of the procedure described in (10) and of that used to obtain homogeneous preparations of recombinant spinach Fd-I (11). Ten grams of cell paste was resuspended in 25 mL of 25 mM potassium phosphate buffer, pH 7.5, containing 0.1 M NaCl (buffer A) and homogenized by sonication (5  $\times$  30 s). After centrifugation at 18888g in a Sorval SS34 rotor for 20 min, the crude extract was loaded onto a (2.5  $\times$  12 cm) DEAE-cellulose column equilibrated in buffer A. After removal of unbound protein with buffer A, Fd was eluted with buffer A containing 0.5 M NaCl. Fractions were pooled on the basis of the brown-red color, diluted 4-fold with 25 mM potassium phosphate buffer, pH 7.5, and loaded on a second (2.5  $\times$  12 cm) DEAE-cellulose column in buffer A. Fd was eluted by applying a 500 mL gradient from 0.1 to 0.5 M NaCl in 25 mM potassium phosphate buffer, pH 7.5. Fd-containing fractions eluted at approximately 0.4 M NaCl and were again pooled on the basis of the brown-red color and were concentrated by ultrafiltration in an Amicon concentrator equipped with a YM3 membrane. At this stage Fd preparations, which are routinely used for Fd-GltS activity assays, were strongly contaminated with nucleic acids as shown by the position

<sup>2</sup> Mass was calculated using the ProtParam tool found at [www.expasy.ch](http://www.expasy.ch) by taking into account posttranslational processing of *glsF* and *gltB* gene products, which cleaves 36 and 42 residue long propeptides, respectively (4). The mature *gltD* gene product was assumed to be processed by removal of the N-terminal methionine residue as in the case of the *Azospirillum*  $\beta$  subunit (37).

Scheme 2: Details of the Partial Reactions Taking Place within Ab-GltS  $\alpha$  Subunit or Fd-GltS<sup>a</sup>

<sup>a</sup> The oxidized and reduced FMN cofactor is represented by the gray and white ovals, respectively. Reactions: a, L-Gln binding; b, L-Gln hydrolysis; c, ammonia transfer from the GAT to the glutamate synthase site; d, formation of the 2-iminoglutarate (2-IG) intermediate; e, reduction of 2-IG to yield the L-Glu product.

of the absorbance maximum in the UV ( $\lambda_{\text{max}} = 257 \text{ nm}$ ) and the high UV/vis absorbance ratio ( $A_{257}/A_{422} \approx 50$ ). Therefore, a 15 mg protein sample was diluted 4-fold to lower its ionic strength and loaded onto a (1.1  $\times$  11 cm) Q-Sepharose anion-exchange column equilibrated in 25 mM Hepes/KOH buffer, pH 7.5. Nitrogen was bubbled in buffers used for chromatographies to decrease dissolved oxygen concentration. Unbound and weakly bound material mainly absorbed at 260 nm and was eluted by washing the column with the equilibrating buffer and with the same buffer containing 200 mM NaCl. A linear 200–600 mM NaCl gradient (100 mL) in the equilibrating buffer was then applied. Fractions containing Fd were eluted at approximately 0.4 M NaCl. They were pooled on the basis of their  $A_{254}/A_{276}$  ratio ( $<1.4$ ) and brought to 1.5 M ammonium sulfate by dilution with an equal volume of 25 mM Hepes/KOH buffer, pH 7.5, containing 3 M  $(\text{NH}_4)_2\text{SO}_4$ . Aliquots of 2–5 mL (containing approximately 1.3–3.25 mg of ferredoxin) were loaded onto a phenyl-Superose HR 5/5 (Pharmacia) column equilibrated with 25 mM Hepes/KOH buffer, pH 7.5, and 1.5 M  $(\text{NH}_4)_2\text{SO}_4$  and connected to an FPLC apparatus (Pharmacia). After the column was rinsed with 5–15 mL of equilibrating buffer at 0.5 mL/min, ferredoxin was eluted by decreasing the  $(\text{NH}_4)_2\text{SO}_4$  concentration to 0 M over a period of 30 min (15 mL). Fractions (1 mL) eluted at approximately 1.2 M  $(\text{NH}_4)_2\text{SO}_4$  contained Fd. They were pooled on the basis of the  $A_{254}/A_{276}$  ratio ( $<0.74$ ), concentrated by ultrafiltration in an Amicon apparatus equipped with a YM3 membrane, and loaded onto a (1.5  $\times$  110 cm) Sephadex G75 gel filtration column equilibrated in 25 mM Hepes/KOH, pH 7.5. Fractions with a  $A_{254}/A_{276}$  ratio  $<0.72$  were pooled, concentrated by ultrafiltration, and stored under nitrogen at  $-80^\circ\text{C}$  after rapid freezing in liquid nitrogen.

**Protein and Activity Measurements.** The protein concentration of purified samples was determined by the Bradford method (12) with bovine serum albumin as the reference protein. For Fd-GltS, a mass of 165476 was used for calculations.<sup>2</sup> Ab-GltS and Ab-GltS  $\alpha$  subunit concentrations were determined using the known extinction coefficients of the enzymes [ $\epsilon_{444} = 62660 \text{ M}^{-1} \text{ cm}^{-1}$  for Ab-GltS (13) and  $\epsilon_{440} = 21200 \text{ M}^{-1} \text{ cm}^{-1}$  for GltS  $\alpha$  subunit (7)]. The *Synechocystis* Fd concentration was calculated, initially, with the Bradford protein assay and a mass of 10363 using sequence ssl0020 deposited in the CyanoBase or the extinction coefficient at 422 nm of  $9700 \text{ M}^{-1} \text{ cm}^{-1}$  used previously (9). Assays of Ab-GltS glutamine-dependent glutamate synthase activity and of GltS  $\alpha$  subunit L-glutamate:iodonitro-

tetrazolium (INT) oxidoreductase activity were carried out as described (6, 7). Fd-GltS activity could also be monitored through its L-glutamate:iodonitrotetrazolium oxidoreductase activity under conditions similar to those used for GltS  $\alpha$  subunit (7). Polyacrylamide gel electrophoresis in the presence of sodium dodecyl sulfate (14) was carried out on 10% or 12% minigels (for Fd-GltS) and 15% minigels (for Fd).

**Determination of Extinction Coefficient, Flavin and Iron Content of Fd-GltS, and Reevaluation of the Extinction Coefficient of Ferredoxin.** The extinction coefficient of *Synechocystis* Fd-GltS was calculated from absorbance spectra of samples (5–10  $\mu\text{M}$ ) that had been gel filtered on a Sephadex G25 column equilibrated in 25 mM Hepes/KOH, pH 7.5, 1 mM EDTA, and 10% glycerol or in 10 mM Hepes/KOH, pH 7.5. On the same Fd-GltS sample, protein concentration was determined with the Bradford method (12), and absorbance and flavin fluorescence emission spectra were recorded. Enzyme cofactors were released from the protein by incubation at  $100^\circ\text{C}$  in the dark, by incubation at the same temperature in the presence of 10% (w/v) trichloroacetic acid (TCA) and 7.5 mM ascorbic acid (15, 16), or by incubation for 1 h on ice in the presence of 10% (w/v) TCA and 7.5 mM ascorbic acid. Denatured protein was removed by centrifugation, and the absorbance spectrum of the resulting free FMN solution was recorded. FMN concentration was calculated using known extinction coefficients ( $\epsilon_{446} = 12200 \text{ M}^{-1} \text{ cm}^{-1}$  for samples at pH 7.5 or  $\epsilon_{446} = 11100 \text{ M}^{-1} \text{ cm}^{-1}$  for samples under acidic conditions; 15 and 16). Supernatants obtained after heat denaturation under acidic conditions were also used for chemical analysis of iron content (15). Samples of released cofactors obtained from heat denaturation of the protein under neutral conditions were instead used for the identification of the flavin cofactor as FMN by comparing the intensity of flavin emission fluorescence before and after addition of phosphodiesterase (16). A solution of authentic FMN (approximately 10  $\mu\text{M}$ ) was also treated under the same conditions as the protein samples and served as a control.

The extinction coefficient of recombinant *Synechocystis* ferredoxin was reevaluated. The absorbance spectrum of a homogeneous ferredoxin solution ( $0.33 \pm 0.06 \text{ mg/mL}$  or  $31.6 \pm 5.3 \mu\text{M}$  according to the Bradford method; 12) in 25 mM Hepes/KOH buffer, pH 7.5, was recorded. Iron was released by addition of 10% TCA and 7.5 mM ascorbic acid and incubation at  $100^\circ\text{C}$  for 10 min (15), denatured protein was removed by centrifugation, and the supernatant was used to determine iron concentration. Ferredoxin concentration in



the initial solution was estimated to be  $31.8 \pm 0.8 \mu\text{M}$  from the iron determination, after correction for dilution, by assuming that it contains one  $[\text{2Fe-2S}]$  cluster per polypeptide chain. The latter value, which agreed well with protein concentration estimated by the Bradford method, was used to calculate the protein extinction coefficient at 424 nm ( $10886 \pm 260 \text{ M}^{-1} \text{ cm}^{-1}$ ) from the absorbance spectrum that had been previously recorded. Such value is in good agreement with that of  $9700 \text{ M}^{-1} \text{ cm}^{-1}$  employed previously (9) and was used throughout this work to estimate Fd concentration.

**Steady-State Kinetic Analysis of the L-Glutamate:Iodonitrotetrazolium Oxidoreductase Activities of Fd-GltS, Ab-GltS, and Ab-GltS  $\alpha$  Subunit.** The steady-state kinetic parameters  $V$  and  $K$  of the L-glutamate:iodonitrotetrazolium oxidoreductase activity exhibited by Fd-GltS, Ab-GltS, and GltS  $\alpha$  subunit were determined spectrophotometrically by measuring the increase of absorbance at 490 nm ( $\epsilon_{490} = 18500 \text{ M}^{-1} \text{ cm}^{-1}$ ) in 1 mL reaction mixtures containing varying concentrations of L-glutamate and iodonitrotetrazolium at 25 °C as previously described (7). Prior to each experiment enzyme solutions were gel filtered through Sephadex G25 (medium) columns equilibrated in 25 mM Hepes/KOH, pH 7.5, 1 mM EDTA, and 10% glycerol. Reaction buffers differed depending on the desired pH value (indicated in parentheses along with their  $\text{pK}_a$  values at 25 °C; 17) and were Hepes ( $\text{pK}_a$  7.5, pH 6.5–8.5), CHES ( $\text{pK}_a$  9.3, pH 8–9), and CAPS ( $\text{pK}_a$  10.4, pH 8.5–10.5). The acidic form of the buffers was titrated to the desired pH value with KOH solutions, and ionic strength in the assays was kept constant at 50 mM by adding suitable amounts of concentrated KCl solutions. Initial velocity values calculated at constant concentration of one of the substrates and varying concentration of the other were fitted to the Michaelis–Menten equation (eq 1) after analysis of double reciprocal plots (eq 2) allowed us to determine deviations from linearity, if any (18).

$$v = (VA)/(K_A + A) \quad (1)$$

$$1/v = 1/V + (K_A/V)(1/A) \quad (2)$$

$$v = VAB/(K_B A + K_A B + AB) \quad (3)$$

In these equations,  $v$  is the initial velocity measured at a given substrate (A) concentration in the presence of a fixed constant level of the second substrate (B),  $K$  is the apparent (or extrapolated, in eq 3)  $K_m$  value for the indicated substrate, and  $V$  is the apparent (or extrapolated, in eq 3) maximum velocity.

When L-Glu was varied in the presence of different constant levels of INT, the steady-state kinetic mechanism describing the reaction was determined by analyzing double reciprocal plots that in all cases yielded parallel lines. Therefore, data were fitted to the equation describing a ping-pong mechanism (eq 3) to obtain estimates of  $V$ ,  $K_{\text{L-Glu}}$ , and  $K_{\text{INT}}$  values extrapolated at infinite concentrations of all substrates. The Grafit program (Erythacus Software Ltd., U.K.) was used to obtain estimates of the kinetic parameters and of their associated errors. When necessary, propagation of statistical error was carried out as described (19).

**Determination of L-Glutamine-Dependent Glutamate Synthase Activity of Fd-GltS.** Fd-GltS ( $2\text{--}5 \mu\text{M}$ ) and, as control samples, Ab-GltS or GltS  $\alpha$  subunit were incubated in 50 mM Hepes/KOH buffer, pH 7.5, in the presence of L-glutamine, 2-oxoglutarate, dithionite, methyl viologen, or ferredoxin in various combinations in 125  $\mu\text{L}$  at room temperature. In different experiments L-[U- $^{14}\text{C}$ ]glutamine (Amersham, 51000 dpm/nmol in experiments at low L-glutamine concentration or 7300 dpm/nmol in experiments at high L-glutamine concentration) or 2-[1- $^{14}\text{C}$ ]oxoglutarate (NEN, 8200 dpm/nmol) was used. Unless otherwise indicated, assays were carried out under anaerobiosis, which was obtained by setting up reaction mixtures lacking dithionite and protein in reactives sealed with a Teflon septum. The solutions were made anaerobic by bubbling oxygen-free nitrogen (20) into them for 20 min. Dithionite (from an anaerobic 100 mM solution in 25 mM Hepes/KOH buffer, pH 7.5, 1 mM EDTA, and 10% glycerol; 20) and/or protein was (were) added, and the reaction was allowed to proceed for 30 min in the dark with nitrogen flowing on its surface. Analysis of the reaction products formed was carried out by loading a 100  $\mu\text{L}$  aliquot of the reaction mixture on a 1 mL Dowex 1-X8 column (acetate form) equilibrated with water (7). The column was eluted with six 1 mL aliquots of water and six 1 mL aliquots of 0.3 M acetic acid. Under these conditions L-glutamine elutes with water and L-glutamate with 0.3 M acetic acid. Quantification of radioactive species was performed by counting of the 1 mL fractions in a Packard Tri-Carb 2 100TR scintillation counter after addition of 5 mL of Ultima Gold (Packard) scintillation fluid. In a separate set of experiments, separation of the reaction components was done by chromatography of the assay mixture on a Mono Q column connected to an FPLC apparatus (Pharmacia) by using the procedure initially designed to separate pyridine nucleotides (21). The column was equilibrated with 10 mM triethanolamine/HCl, pH 7.7. It was run at 1 mL/min, and 1 mL fractions were collected. After sample injection, the column was rinsed with 4 mL of equilibrating buffer. A linear 30 mL gradient from 0 to 0.1 M KCl in the same buffer was then applied, and it was followed by a 10 mL linear gradient from 0.1 to 0.2 M KCl and a 3 mL gradient up to 1 M KCl. Under these conditions L-glutamine was eluted in fractions 2 and 3, L-glutamate in fractions 5 and 6, and 2-oxoglutarate in fractions 26–28.

**Inhibition Studies of Fd-GltS by 6-Diazo-5-oxo-L-norleucine.** Experiments were carried out in several ways. In a first series of experiments Fd-GltS (approximately 560 pmol) was preincubated for 15 min at room temperature in assay mixtures lacking one or more of the components in the presence or absence of 6-diazo-5-oxo-L-norleucine (L-DON, 125 nmol). Anaerobiosis was performed by bubbling nitrogen in the solution prior to the addition of proteins and dithionite as described above. Reaction was started by the addition of the components missing from the assay mixture and L-[U- $^{14}\text{C}$ ]glutamine. Final reagent concentrations in 125  $\mu\text{L}$  assay mixtures were 50 mM Hepes/KOH buffer, pH 7.5, 2.36 mM L-[U- $^{14}\text{C}$ ]glutamine (7300 dpm/nmol), 2.5 mM 2-oxoglutarate, 4 mM dithionite, 0.4 mM methyl viologen or 10  $\mu\text{M}$  ferredoxin, and 4.5  $\mu\text{M}$  Fd-GltS. After incubation at room temperature for 30 min in the dark, quantification of L-glutamine and L-glutamate was performed after chromatographic separation on the Dowex 1-X8 columns as described

above. In a second set of experiments concentrated Fd-GltS (approximately 40  $\mu\text{M}$ ) was incubated in the presence (1 mM) or absence of L-DON and 2-OG (1.1 mM), Fd (approximately 100  $\mu\text{M}$ ), or dithionite (7 mM) in various combinations. Aliquots of the incubation mixture were transferred to an anaerobic complete assay containing 50 mM Hepes/KOH buffer, pH 7.5, 2.36 mM L-[U- $^{14}\text{C}$ ]glutamine (7300 dpm/nmol), 2.5 mM 2-oxoglutarate, 4 mM dithionite, and 0.4 mM methyl viologen or 10  $\mu\text{M}$  ferredoxin. Fd-GltS concentration in the assay was 4–5  $\mu\text{M}$ . Conversion of L-glutamine into L-glutamate was determined after Dowex chromatography and liquid scintillation counting as described above. To distinguish between reversible inhibition by L-DON, due to simple competition with L-glutamine, and irreversible enzyme inactivation, a third protocol was set up. Fd-GltS (approximately 40  $\mu\text{M}$ ) was incubated in the presence of various combinations of 2-oxoglutarate, ferredoxin, and dithionite in 25 mM Hepes/KOH buffer, pH 7.5, 10% glycerol, and 1 mM EDTA as described above. Incubation mixtures (20  $\mu\text{L}$ ) were made anaerobic, if necessary, by blowing nitrogen on their surface for 15 min prior to addition of protein and dithionite. After incubation with L-DON for 15 min, solutions were loaded on Bio-Spin-6 (Bio-Rad) columns (22) that had been equilibrated with 25 mM Hepes/KOH buffer, pH 7.5, 10% glycerol, and 1 mM EDTA. After centrifugation for 4 min at 1000g in a Heraeus Labofuge 400 centrifuge equipped with a 8172 swing-out rotor, elution of protein was effected by washing the column with four 20  $\mu\text{L}$  buffer aliquots. Under these conditions, greater than 95% of the enzyme eluted in the second and third 20  $\mu\text{L}$  fraction, well separated from the low molecular weight material. The enzyme-containing fractions were pooled, enzyme was quantified by both the Bradford protein assay and the L-glutamate:iodonitrotetrazolium activity assay, and approximately 20  $\mu\text{L}$  aliquots were added to anaerobic complete assay mixtures (125  $\mu\text{L}$ ).

**Absorbance and Fluorescence Spectroscopies.** UV/vis absorbance spectroscopy studies were carried out using a Hewlett-Packard HP8453 diode array spectrophotometer at 20 °C. Titrations were done using standard procedures, and anaerobiosis was achieved following the method of Williams et al. (20) as described in recent work on Ab-GltS and GltS  $\alpha$  subunit (2). Differential spectroscopy was carried out using a two-compartment quartz cell. Data were acquired and analyzed with a HP UV/vis Chem Station A.02.05 run on a HP Vectra XA personal computer. Excel (Microsoft) and Grafit 4.0 (Erythacus Software Ltd.) programs were also used for data analysis.

Dissociation constants of the enzyme–sulfite and enzyme–2-oxoglutarate complexes were measured by fitting fractional absorbance changes observed in the presence of different ligands concentrations ([L]) to eq 4, which describes the reversible binding of a ligand to its single binding site on the enzyme:

$$(A_0 - A_x)/(A_0 - A_{\text{fin}}) = [L]/(K_d + [L]) \quad (4)$$

where  $A_0$  is the initial absorbance at a given wavelength,  $A_x$  is the absorbance at a given ligand concentration,  $A_{\text{fin}}$  is the absorbance at the end point of the titration, and  $K_d$  is either the dissociation constant of the enzyme–ligand complex (e.g., in the case of a sulfite titration of the free enzyme) or

the apparent dissociation constant of the enzyme–ligand complex (e.g., for the 2-oxoglutarate titration of the enzyme in the presence of sulfite). In the latter case, the relation between the apparent dissociation constant of the enzyme–2-oxoglutarate complex ( $K_{2\text{-OG,app}}$ ) measured in the presence of sulfite and the actual dissociation constant of the enzyme–2-oxoglutarate complex ( $K_{2\text{-OG}}$ ) is given by the equation:

$$K_{2\text{-OG,app}} = K_{2\text{-OG}}(1 + [\text{sulfite}]/K_{\text{sulfite}}) \quad (5)$$

where  $K_{\text{sulfite}}$  is the dissociation constant of the enzyme–sulfite complex measured during the titration of the free enzyme.

Equation 4 was also used to calculate the equilibrium constant of the reaction between Ab-GltS and L-glutamate. As detailed in the Results section, in this reaction only the FMN cofactor of Ab-GltS is reduced by L-glutamate, which in turn is converted to 2-oxoglutarate and ammonia (23). In this case, fractional absorbance changes correspond to the fraction of enzyme-bound FMN hydroquinone ( $\text{FMN}_{\text{hq}}$ );  $K_d$  corresponds to total added L-glutamate concentration at which 50% of the enzyme flavin has been reduced, with conversion of an equimolar amount of L-glutamate into 2-OG and ammonia. Thus, if  $x$  is such glutamate concentration and  $[\text{E-FMN}]$  is the total enzyme concentration, the equilibrium constant of the reaction  $\text{E-FMN}_{\text{ox}} + \text{L-Glu}$  to yield  $\text{E-FMN}_{\text{red}} + 2\text{-OG} + \text{NH}_3$  can be calculated as

$$\begin{aligned} K_{\text{eq}} &= ([\text{E-FMN}_{\text{red}}][2\text{-OG}][\text{NH}_3])/ \\ &([\text{E-FMN}_{\text{ox}}][\text{L-Glu}]) = (0.5[\text{E-FMN}])^3/ \\ &((0.5[\text{E-FMN}](x - 0.5[\text{E-FMN}])) = (0.5[\text{E-FMN}])^2/ \\ &(x - 0.5[\text{E-FMN}]) \quad (6) \end{aligned}$$

From the known equilibrium constant, the temperature of 20 °C (293.15 K) used in these experiments, the relations between  $K_{\text{eq}}$ ,  $\Delta G^\circ$ , and  $\Delta E^\circ$ , and the known  $E_m$  value of the  $(\text{NH}_3 + 2\text{-OG})/\text{L-glutamate}$  couple ( $E_{m,2} = -0.126$  V; 24), it is possible to calculate the midpoint potential value of the  $\text{E-FMN}_{\text{ox}}/\text{E-FMN}_{\text{red}}$  couple ( $E_{m,1}$ ):

$$\begin{aligned} \Delta E^\circ &= \\ 2.303(RT/nF) \log K_{\text{eq}} &= 0.0281 \log K_{\text{eq}} = (E_{m,1} - E_{m,2}) \quad (7) \end{aligned}$$

with  $R$ , the gas constant (1.9872 cal K $^{-1}$  mol $^{-1}$ ),  $T$ , the absolute temperature (293.15 K),  $n$ , the number of transferred electrons (2), and  $F$ , the Faraday constant (23062.62 cal V $^{-1}$  mol $^{-1}$ ).

Fluorescence spectroscopy was performed with a Jasco FP777 spectrofluorometer at 20 °C. Flavin emission at 530 nm was measured by exciting samples with light at 440 nm. Protein fluorescence emission was measured at 335 nm on samples excited with light at 280 nm.

## RESULTS AND DISCUSSION

**Spectroscopic Properties of Fd-GltS.** The absorbance spectrum of *Synechocystis* Fd-GltS (Figure 1) is very similar to that of Ab-GltS  $\alpha$  subunit with maxima at 278, 370, and 438 nm. The  $A_{278}/A_{438}$  ratio of homogeneous preparations of Fd-GltS is approximately 7.5, similar to the  $A_{278}/A_{440}$  ratio of 7.0 found for Ab-GltS  $\alpha$  subunit (7). The calculated extinction coefficient at 438 nm is  $24380 \pm 1170 \text{ M}^{-1} \text{ cm}^{-1}$

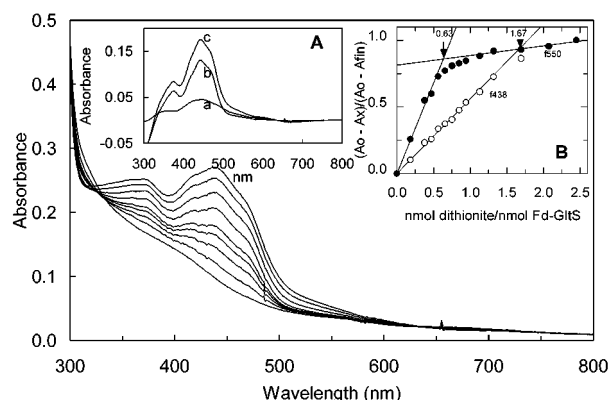


FIGURE 1: Dithionite titration of Fd-GltS. A  $10.8 \mu\text{M}$  solution of Fd-GltS ( $12.8 \text{ nmol}$ ) in  $25 \text{ mM}$  Hepes/KOH buffer, pH 7.5,  $1 \text{ mM}$  EDTA, and  $10\%$  glycerol was made anaerobic and titrated with an anaerobic dithionite solution ( $1.23 \text{ mM}$ ) in the same buffer. Main panel: Absorption spectra of the Fd-GltS solution recorded after the addition of 0, 0.19, 0.38, 0.66, 0.94, 1.13, 1.32, 1.7, and 2.5 dithionite/Fd-GltS molar ratio. Inset A: Differences between spectra recorded after the indicated dithionite additions (mol/mol of Fd-GltS): spectrum a, 0–0.47; spectrum b, 0.47–2.5; spectrum c, 0–2.5. Inset B: Open circles, fractional absorbance changes at  $438 \text{ nm}$  as a function of dithionite/Fd-GltS molar ratio. The lines intersecting at 1.67 are the best fit to points obtained up to 1.32 dithionite/Fd-GltS molar ratio and above 2 dithionite/Fd-GltS molar ratio, respectively. Closed circles, fractional absorbance changes observed at  $550 \text{ nm}$  throughout the titration. The lines intersecting at 0.63 dithionite/Fd-GltS molar ratio are the best fit of points obtained up to 0.47 dithionite/Fd-GltS molar ratio and above 1.32 dithionite/Fd-GltS molar ratio, respectively.

(five determinations), slightly higher than the value of  $21200 \pm 1100 \text{ M}^{-1} \text{ cm}^{-1}$  calculated for GltS  $\alpha$  subunit (7).

Fluorescence measurements of Fd-GltS and of FMN released after heat denaturation of the enzyme showed that flavin fluorescence is quenched approximately 18-fold in Fd-GltS. This value is of the same order of magnitude of that observed for GltS  $\alpha$  subunit (13-fold quenching; 7).

The stoichiometry of FMN and iron bound to Fd-GltS was found to be  $0.88 \pm 0.08 \text{ mol/mol}$  of enzyme (three determinations) and  $2.9 \pm 0.2 \text{ mol/mol}$  of enzyme (three determinations), respectively, when the protein concentration was calculated with the Bradford method (12). These values are in good agreement with the expected values of 1 FMN and 3 non-heme iron atoms bound per Fd-GltS subunit and ensure that the calculated extinction coefficient of Fd-GltS, which was also determined using the protein concentration determined with the Bradford method, is valid.

**Sulfite Reactivity of Fd-GltS.** Ab-GltS holoenzyme and its isolated  $\alpha$  subunit undergo well-defined absorbance changes in the visible region upon reaction with sulfite (7, 15). Such changes are consistent with the formation of covalent addition products between the flavin N(5) atom and sulfite (25). 2-Oxoglutarate was found to displace sulfite from the enzyme flavin in a competitive fashion, suggesting that binding of 2-OG occurs in proximity of the flavin cofactor, a hypothesis that was fully confirmed by structural data (3).

To test the similarity of FMN environment and 2-OG binding among GltS, the interaction between sulfite and recombinant Fd-GltS was studied along with the effect of 2-oxoglutarate on the enzyme–sulfite complex. Titration of a Fd-GltS solution with sulfite led to absorbance changes consistent with formation of the FMN–N(5)–sulfite addition product with a calculated  $K_d$  value of  $10.7 \pm 0.3 \text{ mM}$  for

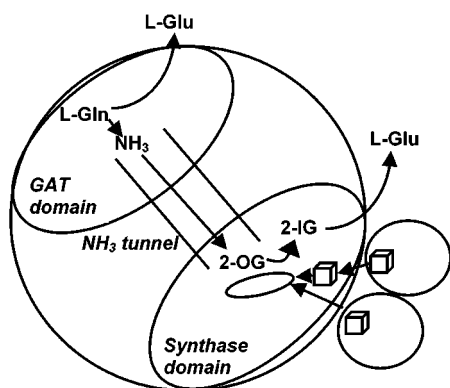
the Fd-GltS–sulfite complex. This value is 5–10-fold higher than those determined for Ab-GltS [ $1.28 \pm 0.07 \text{ mM}$  for the enzyme prepared from *Azospirillum* cells (15) and  $1.52 \pm 0.17 \text{ mM}$  for the recombinant Ab-GltS (H. Stabile and M. A. Vanoni, unpublished)] and for GltS  $\alpha$  subunit ( $2.7 \pm 0.3 \text{ mM}$ ; 7). Back-titration of Fd-GltS in the presence of sulfite with 2-OG caused recovery of the spectrum of the free enzyme. Calculation of the  $K_d$  value for the Fd-GltS–2-OG complex from the apparent dissociation constant of  $0.11 \text{ mM}$  through eq 5 yielded a value of  $17.4 \mu\text{M}$ , which is of the same order of magnitude of that measured for Ab-GltS [ $\approx 6 \mu\text{M}$  for native Ab-GltS (15) and  $\approx 17 \mu\text{M}$  for the recombinant species (H. Stabile and M. A. Vanoni, unpublished)] and for GltS  $\alpha$  subunit ( $34 \mu\text{M}$ ; 7) but significantly lower than the  $K_m$  value determined kinetically on this enzyme ( $0.6 \text{ mM}$ ; 4).

Overall, the FMN environment and the 2-OG binding site of Fd-GltS appear to be similar, although not identical, to those of the Ab-GltS holoenzyme and of its  $\alpha$  subunit, in agreement with the similar primary structure of Fd-GltS and of Ab-GltS  $\alpha$  subunit.

**Dithionite Titrations of Fd-GltS.** Fd-GltS solutions ( $5$ – $11 \mu\text{M}$ ) in  $25 \text{ mM}$  Hepes/KOH, pH 7.5,  $1 \text{ mM}$  EDTA, and  $10\%$  glycerol were made anaerobic and titrated with anaerobic dithionite solutions ( $1$ – $3 \text{ mM}$ ) in the same buffer. The results of one of these experiments are shown in Figure 1. Overall, approximately 1.7 mol of dithionite per mol of Fd-GltS was calculated to be sufficient to fully reduce the enzyme cofactors (Figure 1B), out of which 0.6 was estimated to be necessary for cluster reduction and the remaining 1.1 for flavin reduction. These values are close to the theoretical ones of 0.5 and 1. At variance with the results of similar experiments carried out with the bacterial Ab-GltS holoenzyme and Ab-GltS  $\alpha$  subunit (2, 6, 7), reduction of the Fd-GltS  $[3\text{Fe-4S}]$  cluster preceded that of FMN (Figure 1A,B). In particular, the addition of approximately 0.5 mol of dithionite/mol of Fd-GltS brought about approximately 70% reduction of the iron–sulfur cluster as judged from the comparison of absorbance changes at  $550 \text{ nm}$ , which monitor the extent of iron–sulfur cluster reduction, with those at  $438 \text{ nm}$ , which reflect reduction of both the flavin and the iron–sulfur center (Figure 1B). Subsequent additions of dithionite caused full reduction of both the iron–sulfur cluster and the enzyme flavin (Figure 1A,B). These results were unexpected since midpoint potential values of the cofactors of spinach Fd-GltS have been reported to be similar to each other with values of  $-180 \pm 10 \text{ mV}$  (26) or  $-225 \pm 10 \text{ mV}$  for both the  $\text{FMN}_{\text{ox}}/\text{FMN}_{\text{hq}}$  and  $[3\text{Fe-4S}]^{+1}/[3\text{Fe-4S}]^0$  couples (27).

From the results of the present redox titrations (Figure 1), it can be concluded that in the case of *Synechocystis* Fd-GltS the midpoint potential value of the  $[3\text{Fe-4S}]^{+1}/[3\text{Fe-4S}]^0$  couple is at least 40–50 mV more positive than that of the  $\text{FMN}_{\text{ox}}/\text{FMN}_{\text{hq}}$  couple. A value for the midpoint potential of the  $\text{FMN}_{\text{ox}}/\text{FMN}_{\text{hq}}$  couple of *Synechocystis* Fd-GltS of  $-200 \pm 25 \text{ mV}$  has been calculated from absorbance-monitored redox titrations (4). Thus, it can be calculated that the midpoint potential value of the  $[3\text{Fe-4S}]^{+1}/[3\text{Fe-4S}]^0$  couple in the cyanobacterial enzyme is in the  $-160$  to  $-150 \text{ mV}$  range. That the midpoint potential values of the cofactors of Fd-GltS are less negative than those of Ab-GltS  $\alpha$  subunit was confirmed during two preliminary redox titrations of



Scheme 3: Proposed Electron-Transfer Pathway in Fd-GltS<sup>a</sup>

<sup>a</sup>The two ferredoxin molecules and their [Fe-S] clusters are represented as small spheres and cubes, respectively. The order of binding of the two reduced ferredoxin molecules is not known.

the enzyme in the presence of phenosafranine ( $E_m = -266$  mV at pH 7.5; 28) and anthraquinone-2-sulfonate ( $E_m = -255$  mV at pH 7.5; 28) as indicator dyes, methyl viologen as mediator, and dithionite as reductant. Experimental conditions were similar to those used to determine the midpoint potential values of Ab-GltS cofactors (2). With both dyes, reduction of the enzyme preceded that of the dyes, with the [Fe-S] cluster being reduced first.

No formation of flavin semiquinone species was observed throughout the titration nor during enzyme oxidation upon exposure to air. Thus, as in the case of Ab-GltS (2) the  $\text{FMN}_{\text{ox}}/\text{FMN}_{\text{sq}}$  and  $\text{FMN}_{\text{sq}}/\text{FMN}_{\text{hq}}$  couples should be separated by at least 100 mV. By combining this information with the estimates of the midpoint potential values of the  $\text{FMN}_{\text{ox}}/\text{FMN}_{\text{hq}}$  couple of the *Synechocystis* Fd-GltS (4) and of the  $[\text{3Fe-4S}]^{+1}/[\text{3Fe-4S}]^0$  couple derived from it, it appears that distribution of midpoint potentials of the redox centers [i.e.,  $\text{FMN}_{\text{ox}}/\text{FMN}_{\text{sq}}$  ( $\approx -250$  mV) <  $\text{FMN}_{\text{ox}}/\text{FMN}_{\text{hq}}$  ( $\approx -200$  mV) <  $\text{FMN}_{\text{sq}}/\text{FMN}_{\text{hq}}$  ( $\approx -150$  mV)  $\leq [\text{3Fe-4S}]^{+1}/[\text{3Fe-4S}]^0$  ( $\approx -160$  to  $-150$  mV)] is consistent with electron transfer from reduced ferredoxin to  $\text{FMN}_{\text{ox}}$  directly to generate the (unstable)  $\text{FMN}_{\text{sq}}$  species, followed by transfer of a second electron from a second molecule of reduced ferredoxin either directly to  $\text{FMN}_{\text{sq}}$  or, more likely, through the Fd-GltS  $[\text{3Fe-4S}]$  cluster (Scheme 3). The latter electron-transfer scheme would indeed be very similar to that proposed for the Ab-GltS holoenzyme (Scheme 1; 2) and suggests that the  $[\text{4Fe-4S}]$  of the Ab-GltS holoenzyme implicated in electron transfer between the flavins (Scheme 1; 7) functionally replaces that of reduced ferredoxin in Fd-GltS.

**Glutamate Reduction of Fd-GltS.** The study of the reactivity of Fd-GltS with glutamate further confirmed a slightly different redox behavior of the Fd-GltS centers with respect to the same centers in Ab-GltS and its  $\alpha$  subunit (Figures 2 and 3). Fd-GltS ( $8.5 \mu\text{M}$ ,  $9.7 \text{ nmol}$ ) was made anaerobic and was titrated with an anaerobic solution of L-Glu ( $2.5 \text{ mM}$ ). Absorbance changes after each L-Glu addition were sufficiently slow to be detected by recording spectra at different times with the diode array spectrophotometer used for these experiments. In all cases, the end point of the reaction was reached approximately 1 h after L-glutamate addition. Addition of the first  $0.51 \text{ mol}$  of L-Glu/mol of Fd-GltS led to complete reduction of the enzyme  $[\text{3Fe-4S}]$  center

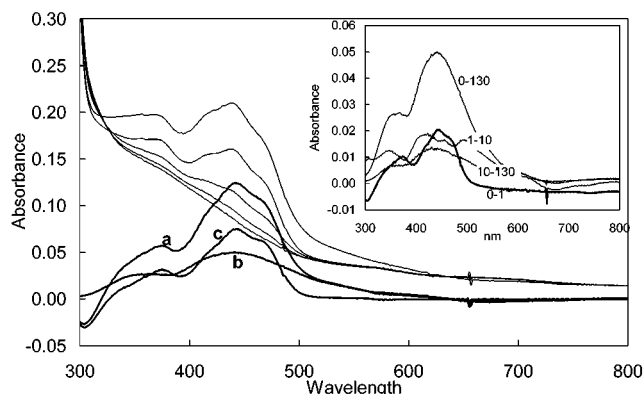


FIGURE 2: L-Glutamate reduction of Fd-GltS. An anaerobic solution of Fd-GltS ( $8.5 \mu\text{M}$ ) was titrated anaerobically with an anaerobic L-glutamate solution ( $2.5 \text{ mM}$ ) in the same buffer. Main panel: Thin lines, top spectrum, oxidized (starting) enzyme; lower spectrum, dithionite-reduced enzyme. Other spectra from bottom: spectra recorded after the addition of 0.51, 1.03, 1.54, and 3.1 mol of L-glutamate/mol of Fd-GltS. Thick lines: difference of spectra recorded after the addition of the indicated amounts of L-glutamate (mol/mol of Fd-GltS). Spectrum: a, 0–3.1; b, 0–0.51; c, 0.51–3.1. The inset shows spectral changes observed at different times after addition of 0.51 mol of L-glutamate/mol of Fd-GltS: 0–130, difference between the spectrum measured before L-glutamate addition and that recorded 130 min after L-glutamate addition and corresponds to spectrum b of the main panel; 0–1, spectral changes observed during the first minute of reaction; 1–10, difference between the spectrum recorded 1 min after glutamate addition and that recorded at 10 min; 10–130, spectral changes observed between 10 and 130 min of reaction.

without detection of flavin semiquinone species as judged by the shape and magnitude of absorbance spectra (Figure 2, main panel, spectrum b). Further L-Glu additions led to absorbance changes consistent with reduction of approximately 90% enzyme flavin (Figure 2, spectrum c). In these and other calculations we assume that flavin reduction brings along an absorbance change of  $10 \text{ mM}^{-1} \text{ cm}^{-1}$  at  $441 \text{ nm}$  (29) which is the maximum of difference spectra. Inspection of spectral changes observed at different time intervals after addition of the first 0.51 equiv of L-glutamate (Figure 2, inset) and of the time course of absorbance changes at 438 and  $550 \text{ nm}$  (Figure 3) revealed that the reaction between Fd-GltS and L-glutamate takes place in distinct phases: in the first minute of reaction 2-electron-reduced FMN builds up (Figure 2, inset); during the following 10 min the iron-sulfur cluster is reduced parallel to flavin reoxidation. Finally, completion of iron-sulfur cluster reduction is observed.

The Fd-GltS behavior was surprising since previous experiments with Ab-GltS indicated that only FMN could be reduced on anaerobic addition of a 10–40-fold molar excess of L-Glu (7). Thus, the experiments were repeated using Ab-GltS and its  $\alpha$  subunit by paying attention to slow absorbance changes following each L-Glu addition.

Titration of Ab-GltS  $\alpha$  subunit with L-glutamate led to absorbance changes, which were completed 2–3 h after each L-Glu addition (not shown). Addition of  $0.35 \text{ mol}$  of L-Glu/mol of GltS  $\alpha$  subunit led to partial reduction of the enzyme  $[\text{3Fe-4S}]$  center. Subsequent L-glutamate additions brought about further  $[\text{Fe-S}]$  cluster reduction and caused complete flavin reduction. The analyses of spectral changes observed at different time intervals after the first L-glutamate addition and of the kinetics of absorbance decrease at 440 and  $550 \text{ nm}$  (Figure 3) confirm that L-glutamate first reduces the

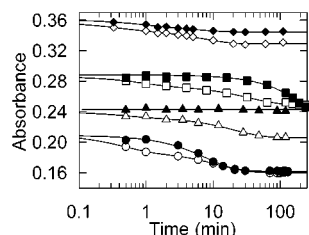


FIGURE 3: Comparison of the reactivities of Fd-GltS, NADPH-GltS  $\alpha$  subunit, and NADPH-GltS holoenzyme with L-glutamate. The kinetics of absorbance changes observed at approximately 440 nm (open symbols) are compared with those observed at 550 nm (closed symbols) upon addition of approximately 0.5 mol of L-glutamate/mol of enzyme. Circles: absorbance changes at 438 and 550 nm recorded after the addition of 0.51 mol of L-glutamate/mol of Fd-GltS (Figure 2). To allow direct comparison, absorbance values at 550 nm have been multiplied by 2.95. The lines correspond to the following functions:  $A_{438} = 0.022e^{-(2.23t)} + 0.027e^{-(0.082t)} + 0.16$  and  $A_{550} = 0.047e^{-(0.126t)} + 0.16$ . Squares: data from an L-glutamate titration of NADPH-GltS  $\alpha$  subunit (13.2  $\mu$ M) after the addition of the first aliquot of L-glutamate (0.35 mol/mol of enzyme).  $A_{550}$  values have been multiplied by 4.4. The lines correspond to the following functions:  $A_{440} = 0.012e^{-(1.16t)} + 0.024e^{-(0.03t)} + 0.25$  and  $A_{550} = 0.102e^{-(0.002t)} + 0.19$ . Triangles: data from an L-glutamate titration of NADPH-GltS holoenzyme (8.2  $\mu$ M) after the first addition of L-glutamate (0.54 mol/mol of enzyme). For graphical purposes,  $A_{550}$  values were multiplied by 4.76, and a value of 0.01 was subtracted; a value of 0.27 was subtracted from  $A_{444}$  values. The curve corresponds to the function  $A_{444} = 0.007e^{-(2.06t)} + 0.027e^{-(0.05t)} + 0.21$ , and a horizontal line was drawn through the  $A_{550}$  value, which did not vary significantly throughout the experiment. Diamonds: absorbance changes observed after addition of 0.6 mol of L-glutamate per mol of Fd-GltS in the presence of ferredoxin (2 mol of ferredoxin/mol of Fd-GltS, Figure 6).  $A_{550}$  values have been multiplied by 2.95. Lines correspond to the following functions:  $A_{438} = 0.010e^{-(2.84t)} + 0.019e^{-(0.15t)} + 0.33$  and  $A_{550} = 0.008e^{-(1.21t)} + 0.008e^{-(0.18t)} + 0.35$ .

enzyme-bound flavin and show that electron transfer from the flavin to the Fe/S cluster is significantly slower than with Fd-GltS. Indeed, during the first 16 min of reaction only flavin reduction is observed. In the following time interval (16–64 min) [Fe–S] cluster reduction seems to take place, but only in the following 2 h is electron transfer from the flavin to the cluster completed.

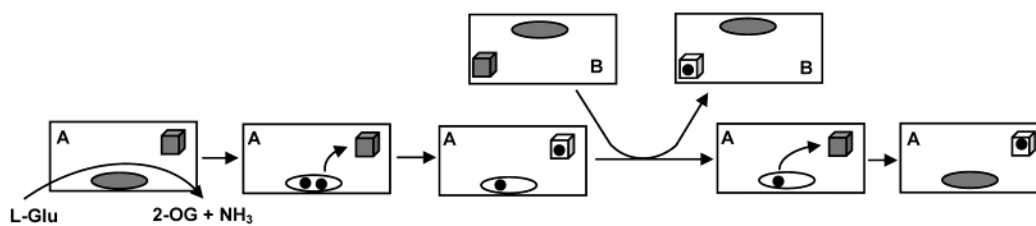
The titration of the Ab-GltS holoenzyme with L-glutamate confirmed that the reaction with L-glutamate was very slow as judged by the fact that it took between 1 and 3 h to reach completion after each glutamate addition. More importantly, the absorbance changes were consistent with reduction of only one enzyme flavin (most likely FMN at the L-glutamate site) with no indication of iron–sulfur cluster reduction (Figure 3). Only after overnight incubation of the enzyme with a 13-fold molar excess of L-glutamate at 20 °C was a small decrease of absorbance at wavelengths above 500 nm observed (not shown), but it was attributed to enzyme denaturation rather than iron–sulfur cluster reduction. Interestingly, the fractional absorbance changes we observed at 440 nm exhibited hyperbolic dependence on the total L-glutamate concentration added. The L-glutamate concentration required to reduce half of the enzyme FMN cofactor was 8.44  $\mu$ M. Since we have previously shown that GltS converts L-glutamate into 2-oxoglutarate and ammonia (23), we could use the known enzyme concentration and midpoint potential value of the (NH<sub>3</sub> + 2-OG)/(L-Glu) couple (−0.126 mV; 24) to obtain an estimate of the midpoint potential of

the Ab-GltS-bound FMN<sub>ox</sub>/FMN<sub>hq</sub> couple. The calculated value (see Experimental Procedures for details) was −278 mV, in good agreement with the value of  $-267 \pm 1.4$  mV calculated from previous reductive titrations of the enzyme in the presence of 2-oxoglutarate (2).

These results lead to several conclusions. It is confirmed that the site of entry of electrons during reaction of GltS with L-glutamate is the enzyme FMN cofactor, as expected. The fact that FMN redox potential is less negative than that of the same cofactor in Ab-GltS may be sufficient to explain why FMN reduction by L-Glu in Fd-GltS is easier (thus faster) than with the Ab-GltS holoenzyme and  $\alpha$  subunit. Electron transfer from the enzyme flavin to the [3Fe–4S] cluster is possible both in Fd-GltS and in GltS  $\alpha$  subunit but not with the Ab-GltS holoenzyme, although it appears to be more facile with Fd-GltS. With the latter enzyme, 0.5 mol of L-glutamate is sufficient to fully reduce 1 mol [Fe–S] cluster/mol of enzyme, and no flavin semiquinone species accumulates during the process. Thus, it must be concluded that both intermolecular and intramolecular electron transfers are possible in Fd-GltS as depicted in Scheme 4. Intramolecular transfer of one electron from FMN<sub>hq</sub> to [3Fe–4S]<sup>+</sup> and intermolecular transfer between [3Fe–4S] clusters are possible as the centers exhibit similar midpoint potentials. The second intramolecular electron transfer from FMN<sub>sq</sub> to [3Fe–4S]<sup>0</sup> may be fast since it may be driven by the large favorable midpoint potential difference between the centers. In Ab-GltS  $\alpha$  subunit the first intramolecular electron transfer from reduced FMN to the oxidized cluster is made difficult by an unfavorable thermodynamic barrier (2), but the possibility of intermolecular electron transfer between [Fe–S] centers on separate molecules allows the detection of such rare event. In the Ab-GltS holoenzyme intramolecular electron transfer between FMN and the [Fe–S] cluster is also opposed by a thermodynamic barrier, and intermolecular electron transfer is prevented by the presence of the  $\beta$  subunit (Scheme 1).

**L-Glutamate:Iodonitrotetrazolium Oxidoreductase Activity of Fd-GltS.** The relatively facile reduction of Fd-GltS by L-glutamate as compared to that of Ab-GltS and of its  $\alpha$  subunit prompted a steady-state kinetic study of the L-Glu:iodonitrotetrazolium oxidoreductase reaction (7) exhibited by the three enzyme species at different pH values. Indeed, all GltS should be devoid of significant L-glutamate oxidizing activities, at least at neutral pH values and at low L-glutamate concentrations, to fulfill its role in cellular ammonia assimilation processes. This was found to be true for the Ab-GltS holoenzyme (23) which can convert L-glutamate into ammonia and 2-oxoglutarate only at basic pH values and with a low efficiency (23). With all three enzymes the initial velocity of reactions carried out at constant substrate concentration (L-Glu, 20 mM, and INT, 0.1 mM) was too low to be detected at pH 6 and increased 10-fold from pH 7.5 to pH 9.5 with a sharp drop above pH 10 (due at least in part to rapid enzyme denaturation as determined in control experiments), confirming previous results with Ab-GltS. The reaction was studied in greater detail at three selected pH values (7.5, 8.5, and 9.5, Table 1). The reaction was in all cases well described by a ping-pong kinetic mechanism. The catalytic efficiency of Fd-GltS was found to be 7-fold higher than that of Ab-GltS at high pH values, mainly due to a 20-fold lower  $K_m$  value for L-glutamate. At pH 7.5 Fd-GltS-



Scheme 4: Intermolecular Electron Transfer in Fd-GltS<sup>a</sup>

<sup>a</sup> Only the synthase domain of Fd-GltS is shown with the FMN cofactor and the [3Fe-4S] cluster indicated as oval and cube, respectively. The oxidized forms of the cofactors are in gray; the reduced forms are in white with electrons indicated as black dots.

Table 1: Comparison of the Steady-State Kinetic Parameters of the L-Glutamate:Iodonitrotetrazolium Oxidoreductase Activity Exhibited by Fd-GltS, NADPH-GltS  $\alpha$  Subunit, and NADPH-GltS Holoenzyme<sup>a</sup>

enzyme	buffer, pH	L-Glu, mM	INT, mM	eq	$V$ , min <sup>-1</sup>	$K_{L-Glu}$ , mM	$K_{INT}$ , mM	$V/K_{L-Glu}$ , min <sup>-1</sup> mM <sup>-1</sup>
Fd-GltS	CAPS, pH 9.5	0.05–2	0.2	1	220 $\pm$ 4	0.044 $\pm$ 0.005		5000 $\pm$ 575
	CAPS, pH 9.5	0.05–1	0.1, 0.2, 0.3	2	186 $\pm$ 7	0.046 $\pm$ 0.004	0.10 $\pm$ 0.01	4043 $\pm$ 383
	Hepes, pH 8.5	0.05–1	0.2	1	129 $\pm$ 4	0.065 $\pm$ 0.01		1985 $\pm$ 311
	Hepes, pH 8.5	0.1–0.5	0.1, 0.14, 0.2, 0.3	2	256 $\pm$ 22	0.085 $\pm$ 0.02	0.33 $\pm$ 0.04	3012 $\pm$ 754
	Hepes, pH 7.5	0.05–1	0.2	1	39 $\pm$ 1	0.133 $\pm$ 0.01		293 $\pm$ 23
NADPH-GltS $\alpha$ subunit	Hepes, pH 7.5	0.1–0.5	0.1, 0.2, 0.3	2	89 $\pm$ 19	0.33 $\pm$ 0.1	0.31 $\pm$ 0.10	270 $\pm$ 100
	CAPS, pH 9.5	1–40	0.1	1	200 $\pm$ 3.5	1.5 $\pm$ 0.1		133 $\pm$ 9
	Hepes, pH 8.5	1–40	0.1	1	130 $\pm$ 1.1	0.92 $\pm$ 0.03		141 $\pm$ 5
	Hepes, pH 7.5	1–40	0.1	1	16 $\pm$ 0.07	0.63 $\pm$ 0.02		25 $\pm$ 1
	CAPS, pH 9.5	1–20	0.1	1	564 $\pm$ 13	0.73 $\pm$ 0.085		773 $\pm$ 92
NADPH-GltS	Hepes, pH 8.5	1–20	0.1	1	178 $\pm$ 1	0.23 $\pm$ 0.016		774 $\pm$ 54
	Hepes, pH 7.5	1–20	0.1	1	20 $\pm$ 0.2	0.23 $\pm$ 0.02		87 $\pm$ 8

<sup>a</sup> Assays were carried out at 25 °C in the indicated buffer (50 mM) and at the stated substrate concentrations or concentration ranges.

catalyzed L-Glu oxidation is still at least 3-fold more efficient than that of Ab-GltS due to a combination of higher turnover number and lower  $K_m$  value. Whether this observation implies a role of Fd-GltS in L-glutamate catabolism in the cell remains to be established. However, these experiments agree with the results of anaerobic L-glutamate titrations of GltS. The efficient L-Glu oxidation reaction catalyzed by Fd-GltS as opposed to Ab-GltS is in full agreement with differences in the midpoint potential values of the FMN cofactor in the three enzyme species.

**Reactivity of Reduced Fd-GltS with L-Glutamine and 2-Oxoglutarate.** During the physiological glutamate synthase reaction of GltS, the ferredoxin- or NADPH-reduced enzyme is proposed to bind L-glutamine and 2-oxoglutarate and to efficiently catalyze the hydrolysis and transfer of ammonia from glutamine to 2-oxoglutarate (Scheme 2). Formation of the postulated 2-iminoglutarate intermediate should be followed by its reduction to L-glutamate with reducing equivalents provided directly by reduced FMN. Accordingly, when the Ab-GltS holoenzyme is fully reduced photochemically and is reacted with a molar excess of L-Gln (or ammonia) and 2-oxoglutarate, full recovery of the spectrum of the oxidized enzyme is obtained within the mixing time of the reagents (0.5 min in the diode array spectrophotometer; ref 30 and H. Stabile and M. A. Vanoni, unpublished). With GltS  $\alpha$  subunit only prompt reoxidation of the FMN cofactor was observed by reacting the dithionite-reduced form with 2-OG and L-glutamine (or ammonia) (7) even in the presence of methyl viologen (used to promote electron transfer between the flavin and the [3Fe-4S] cluster; unpublished). Surprisingly, addition of a 188-fold molar excess each of 2-OG and glutamine from the sidearm of the cuvette to dithionite-reduced Fd-GltS (10  $\mu$ M; Figure 4) led to a slow absorbance increase that took approximately 2 h to reach

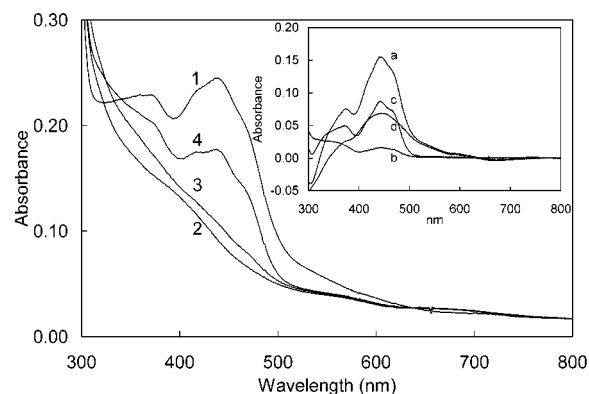


FIGURE 4: Reaction of dithionite-reduced Fd-GltS with L-glutamine and 2-oxoglutarate. A 9.8  $\mu$ M solution of Fd-GltS (13.3 nmol, spectrum 1) was anaerobically reduced by adding 2.5-fold mol of sodium dithionite/mol of Fd-GltS (spectrum 2). L-Glutamine and 2-oxoglutarate (2500 nmol of each) were added from the sidearm of the anaerobic cuvette, and spectra were recorded immediately after mixing with substrate solution (spectrum 3, 1 min after mixing) and repeated at several times after substrate addition until no absorbance changes were observed (193 min, spectrum 4). The inset shows the following difference spectra: spectrum a, spectrum 1 – spectrum 2; spectrum b, spectrum 3 – spectrum 2; spectrum c, spectrum 4 – spectrum 2; spectrum d, spectrum 1 – spectrum 4.

completion (Figure 5) and caused spectral changes consistent with the reoxidation of the enzyme FMN cofactor only (Figure 4 inset, spectrum c). Indeed, full recovery of the spectrum of the oxidized enzyme was obtained by exposure of the solution to air at the end of the experiment. This result suggested that dithionite-reduced Fd-GltS is catalytically impaired in one or more reaction steps, namely, glutamine binding (Scheme 2, a), hydrolysis (b), ammonia transfer from the amidotransferase site to the 2-oxoglutarate site (c), or reduction of the iminoglutarate intermediate formed (d and

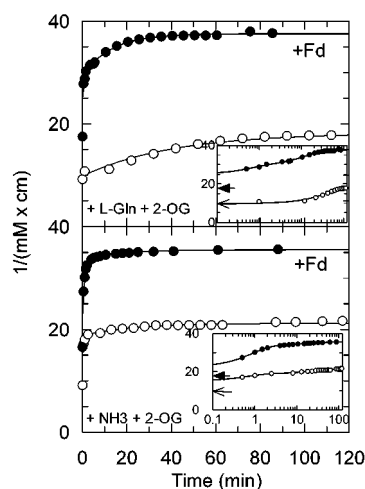


FIGURE 5: Comparison of the kinetics of oxidation of reduced Fd-GltS with 2-oxoglutarate and L-glutamine (or ammonia) and effect of ferredoxin on the reaction. Upper panel: Absorbance values measured at 438 nm during the reaction of dithionite-reduced Fd-GltS with L-glutamine and 2-oxoglutarate in the absence (open symbols, Figure 4) or presence of ferredoxin (closed symbols, Figure 6) were converted to apparent extinction coefficients by dividing them by Fd-GltS concentration (expressed as millimolar). The curves correspond to the following functions: open circles,  $8.4[1 - e^{-(0.025t)}] + 9.8$ ; closed circles,  $4.3[1 - e^{-(1.6t)}] + 8.2[1 - e^{-(0.08t)}] + 25.1$ , which were obtained by fitting the absorbance data to equations describing the sum of one or two exponential processes starting from the value measured at 0.5 min after substrate addition. The inset shows the time course of absorbance changes using a logarithmic time scale. The thin arrow indicates the initial absorbance value of Fd-GltS solution; the thick arrow shows the initial absorbance of the Fd/Fd-GltS solution. The lower panel shows the time course of absorbance changes observed at 438 nm during the reaction of dithionite-reduced Fd-GltS in the absence or presence (2.2 mol/mol of Fd-GltS) of ferredoxin with ammonia (approximately 750 mol/mol of Fd-GltS) and 2-oxoglutarate (approximately 125 mol/mol of Fd-GltS). Normalization and symbols are as described for data presented in the upper panel. The curves correspond to the following functions: open circles,  $3.5[1 - e^{-(1.5t)}] + 2.4[1 - e^{-(0.05t)}] + 15$ ; closed circles,  $10.8[1 - e^{-(1.17t)}] + 2.1[1 - e^{-(0.065t)}] + 22.6$ .

e). Binding of 2-oxoglutarate to the enzyme should not be impaired in the enzyme as shown by the fact that 2-oxoglutarate efficiently (and rapidly) displaces sulfite from the enzyme flavin as observed during our back-titration of the enzyme-sulfite complex with 2-oxoglutarate.

To attempt to detect which step(s) is (are) impaired in free Fd-GltS, we added a 125-fold excess of 2-oxoglutarate and a 780-fold molar excess of ammonia from the sidearm of a cuvette containing Fd-GltS, which had been reduced by addition of a total of 3 mol of dithionite/mol of enzyme (not shown). In this way, we most likely bypassed steps a–c of Scheme 2. As shown in Figure 5, absorbance recovery was significantly faster than observed with L-glutamine + 2-oxoglutarate. The initial rapid phase accounted for the oxidation of approximately half of the enzyme flavin. In the second (slow) phase of absorbance recovery, which was over 40 min after substrate addition, essentially only flavin oxidation took place. Thus, it appears that it is the step(s) involving glutamine binding and hydrolysis and/or ammonia transfer to the 2-oxoglutarate site (steps a–c of Scheme 2) that is (are) mainly impaired in free Fd-GltS.

*Effect of Ferredoxin on the Reactivity of Fd-GltS with L-Glutamine and 2-Oxoglutarate.* The catalytic turnover of

Table 2: Glutamate Synthase Activity of Fd-GltS<sup>a</sup>

dithionite, 4 mM	MV, 0.4 mM	Fd, 10 $\mu$ M	L-[U- <sup>14</sup> C]- Gln, mM	2-OG, 2.5 mM	L-Glu, %	L-Glu, nmol
+	+	–	0.42	+	64	27.0
+	–	+	0.42	+	95	40.0
–	–	+	2.34	+	1.1	2.6
–	–	+	2.34	+	1.3	3.0
+	+	–	2.34	+	18	42.1
+	–	+	2.34	+	88	206.0
dithionite, 4 mM	MV, 0.4 mM	Fd, 10 $\mu$ M	L-Gln, mM	2-[1- <sup>14</sup> C]- OG, 2.2 mM	L-Glu, %	L-Glu, nmol
+	+	–	2.4	+	19	41.8
+	–	+	2.4	+	84	184.8

<sup>a</sup> Experiments were carried out in 50 mM Hepes/KOH buffer, pH 7.5, in a final volume of 125  $\mu$ L and the indicated concentrations of reagents. Fd-GltS concentration was 4.5  $\mu$ M. After 30 min of reaction, the amount of residual L-[U-<sup>14</sup>C]glutamine (51000 dpm/nmol when used at low concentration or 7300 dpm/nmol when used at high concentration) and of L-[1-<sup>14</sup>C]glutamate formed from 2-[1-<sup>14</sup>C]oxoglutarate (8200 dpm/nmol) was determined after chromatography of the reaction mixture on a MonoQ column and liquid scintillation counting, as described in the Experimental Procedures section.

Fd-GltS with glutamine and 2-oxoglutarate has been reported to be significantly higher in the presence of dithionite + ferredoxin than with dithionite + methyl viologen. This observation was also confirmed by us (Table 2) when we monitored the conversion of L-[U-<sup>14</sup>C]glutamine or 2-[1-<sup>14</sup>C]oxoglutarate into <sup>14</sup>C-labeled L-glutamate under various conditions. Therefore, we wished to test if ferredoxin had a stimulatory effect on the reaction between Fd-GltS and its physiological substrates L-glutamine and 2-oxoglutarate. To carry out such experiment, we had to design a procedure which allowed us to remove nucleic acids that contaminate recombinant *Synechocystis* ferredoxin preparations routinely used for activity assays. This goal was achieved as detailed in the Experimental Procedures section. Furthermore, we wished to use the repurified Fd preparations to check the Fd/Fd-GltS dissociation constant value ( $\approx 5 \mu$ M from kinetic measurements; 4) by means of fluorescence or absorbance spectroscopies. Unfortunately, titration of a Fd-GltS solution with concentrated Fd solutions yielded flavin and protein fluorescence changes, as well as absorbance changes, too small to be interpreted.

For the determination of the effect of Fd on the properties of Fd-GltS, we decided to maintain the Fd/Fd-GltS molar ratio between 1.5 and 2.5. We calculated that, with the protein concentrations used during the experiments and a dissociation constant of the Fd/Fd-GltS complex of 5  $\mu$ M (4), greater than 50% of Fd-GltS would be present in the complex with ferredoxin. Thus, a significant fraction of the Fd/Fd-GltS complex would be present in solution, and even small absorbance changes due to Fd-GltS oxidation would not be completely obscured by ferredoxin absorbance.

We first titrated anaerobic solutions of Fd-GltS and Fd by adding aliquots of a concentrated dithionite solution. The presence of ferredoxin did not affect the course of the dithionite titration of Fd-GltS. We observed absorbance changes consistent with reduction of most of the Fd-GltS [3Fe-4S] cluster, followed by reduction of the enzyme flavin as with the free enzyme (Figure 1). Only when most of the flavin had been reduced was slow reduction of Fd observed, consistent with its expected low midpoint potential value

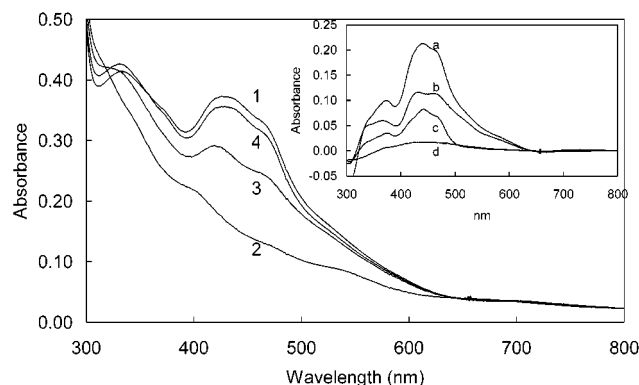


FIGURE 6: Effect of ferredoxin on the reaction of reduced Fd-GltS with L-glutamine and 2-oxoglutarate. A solution containing 9  $\mu$ M Fd-GltS (11 nmol) and 13  $\mu$ M ferredoxin was made anaerobic (spectrum 1). A total of 3.3 mol of sodium dithionite/mol of Fd-GltS was added and was sufficient to fully reduce Fd-GltS and approximately 50% of ferredoxin present (spectrum 2). L-Glutamine and 2-oxoglutarate (1250 nmol of each) were added from the sidearm of the cuvette, and spectra were recorded immediately after mixing (spectrum 3, 0.5 min) and at different times until reaction reached completion (spectrum 4, 90 min). Inset: spectrum a, spectrum 1 – spectrum 2; spectrum b, spectrum 3 – spectrum 2; spectrum c, spectrum 4 – spectrum 3; spectrum d, spectrum 1 – spectrum 4.

( $\leq -0.412$  V at pH 7.5; 31). To avoid the onset of turnover in the next part of the experiment, we interrupted dithionite addition when sufficient reagent had been added (3–4 mol of dithionite/mol of Fd-GltS) to fully reduce Fd-GltS and to reduce approximately 50% of Fd present. As shown in Figures 5 and 6, the experimental set up allowed us to demonstrate a strong stimulatory effect of ferredoxin on the reaction between Fd-GltS and 2-oxoglutarate and L-glutamine. At variance with the reaction observed in the absence of ferredoxin (Figures 4 and 5) the oxidation reaction took place in two distinct phases. The first phase was essentially completed 0.5 min after substrate addition (corresponding to the first spectrum we could record). It clearly showed that ferredoxin had been fully reoxidized (Figure 6 inset, spectrum b). Comparison of the spectra recorded throughout the experiment and the difference spectra shown in the inset of Figure 6 indicates that also most of the Fd-GltS [Fe-S] cluster is being oxidized in this initial rapid phase. Subsequent changes are slower and are mainly associated with flavin oxidation only. A similar experiment was carried out by adding 2-oxoglutarate and ammonia to a dithionite-reduced solution containing Fd and Fd-GltS (not shown). The reaction consisted in oxidation of Fd and (most of) the enzyme [Fe-S] cluster in the first rapid phase and was followed by flavin oxidation, which was completed 40 min after substrate addition (Figure 5). From these experiments it can be concluded that the first fast phase of reaction of reduced Fd-GltS in the presence of reduced Fd is associated with (1) rapid oxidation of the Fd-GltS-reduced FMN cofactor (with the enzyme in complex with reduced ferredoxin) and production of L-Glu from 2-OG and L-Gln (or ammonia), followed by (2) electron transfer from both reduced ferredoxin and the [3Fe-4S] cluster to FMN<sub>ox</sub> yielding the hydroquinone species. The second slow reaction phase reflects slow oxidation of the enzyme (free or in complex with oxidized Fd) as observed in the absence of Fd (Figures 4 and 5).

In conclusion, it seems that reduced ferredoxin bound to Fd-GltS is required to activate glutamine binding, hydrolysis, or ammonia transfer to the 2-oxoglutarate site (steps a–d of Scheme 2) with a milder effect on the reaction involving conversion of the iminoglutarate intermediate into L-glutamate (Scheme 2, e). Furthermore, it is only in the presence of reduced ferredoxin that the enzyme [3Fe-4S] cluster participates at the catalytic turnover, presumably by mediating flavin reduction as depicted in Scheme 3 and discussed above.

**Effect of Fd on Other Properties of Fd-GltS.** The experiments described above demonstrated that binding of Fd to Fd-GltS has a dramatic effect on the catalytic properties of the enzyme by inducing presumably small, but functionally significant, long-range conformational changes. Therefore, we wished to determine the effect of Fd on other properties of Fd-GltS, namely, sulfite reactivity and reaction with L-glutamate, the product of the reaction. Fd had no detectable effect on sulfite reactivity of Fd-GltS ( $K_d$   $14.5 \pm 1.5$  mM). On the contrary, ferredoxin accelerated electron transfer between L-glutamate-reduced FMN and the [3Fe-4S] cluster (Figure 3). After the addition of approximately 0.5 mol of L-Glu/mol of Fd-GltS, absorbance at 438 nm and absorbance at 550 nm decreased almost parallel to each other (Figure 3). Furthermore, it appears that Fd prevents to some extent the intermolecular electron-transfer process between [3Fe-4S] clusters (Scheme 4) so that less [3Fe-4S] cluster is reduced after the addition of 0.5 molar equiv of L-Glu to Fd-GltS in the presence of Fd (not shown) as compared to free Fd-GltS.

**Glutaminase Activity of Fd-GltS.** A key difference between the Ab-GltS holoenzyme and its isolated  $\alpha$  subunit is the ability of the isolated  $\alpha$  subunit to catalyze glutamine hydrolysis in the absence of the other enzyme substrates (7, 23). No glutaminase activity has ever been reported for Fd-GltS. However, we wished to check for the presence or absence of glutaminase activity on the preparations used for the experiments presented here using the method previously employed to demonstrate the presence of glutaminase activity in the GltS  $\alpha$  subunit (7). We first assessed the ability of Fd-GltS to convert L-[U- $^{14}$ C]glutamine in L-[U- $^{14}$ C]glutamate in the presence of 2-oxoglutarate and dithionite + methyl viologen or dithionite + ferredoxin as the reducing system (Table 2). As reported for other Fd-GltS (e.g., refs 4 and 32–34) and for GltS  $\alpha$  subunit (7), dithionite alone is a poor electron donor during catalytic turnover with glutamine and 2-oxoglutarate, while inclusion of methyl viologen is sufficient to support glutamate synthesis. However, the fractional conversion of glutamine into glutamate obtained in the presence of dithionite-reduced ferredoxin was significantly greater than that measured with dithionite + methyl viologen, especially at the higher glutamine concentration used (2.4 mM; Table 2). A similar pattern was observed when 2-[1- $^{14}$ C]oxoglutarate was used as the radioactive substrate (Table 2). To detect glutaminase activity of Fd-GltS, the enzyme was incubated with L-[U- $^{14}$ C]glutamine alone or in the presence of 2-oxoglutarate, dithionite, dithionite + methyl viologen, or dithionite + ferredoxin in various combinations (see, for example, lines 3 and 4 of Table 2). In no case did we detect glutamate production in the absence of one of the components of the glutamate synthase reaction. Similar



Table 3: Inhibition of Fd-GltS by 6-Diazo-5-oxo-L-norleucine<sup>a</sup>

preincubation						assay		
L-DON, mM	Fd-GltS, $\mu$ M	2-OG, mM	Fd, $\mu$ M	dithionite, mM	gel filtration	L-DON, mM	Fd-GltS, $\mu$ M	L-Glu formed, nmol
none	38	—	—	—	—	none	4.2	143
1	38	—	—	—	—	0.112	4.2	37
none	45	1.1	114	6.7	—	0.13	5.3	158
1	45	1.1	114	6.7	—	1.22	5.3	19
none	45	1.1	114	6.7	—	none	5.3	158
none	45	1.1	114	6.7	—	1.1	5.3	32
none	38	—	—	—	+	none	1.5	94
1	38	—	—	—	+	none	1.9	131
none	38	1.25	—	—	+	none	1.6	137
1	38	1.25	—	—	+	none	1.6	136
none	38	1.25	96	—	+	none	2.3	126
1	38	1.25	96	—	+	none	1.9	114
none	38	1.25	96	7	+	none	2.5	138
1	38	1.25	96	7	+	none	2.2	142

<sup>a</sup> Fd-GltS was incubated in 25 mM Hepes/KOH buffer, pH 7.5, 10% glycerol, and 1 mM EDTA in the presence of the indicated reaction components for 15 min. At the end of the preincubation an aliquot of the incubation mixture was transferred to an assay mixture containing 2.32 mM L-[U-<sup>14</sup>C]glutamine (7300 dpm/nmol), 2.5 mM 2-oxoglutarate, 4 mM dithionite, and 10  $\mu$ M Fd. After 30 min the amount of L-glutamate formed was determined after chromatography on a Dowex 1-X8 column and liquid scintillation counting as detailed in the Experimental Procedures section. In a set of experiments, the preincubation mixture was gel filtered through a spun column equilibrated in 25 mM Hepes/KOH, pH 7.5, 1 mM EDTA, and 10% glycerol; the enzyme contained in the first two to three 20  $\mu$ L fractions eluted from the column was quantified and added to an assay mixture as before.

results were obtained with the Ab-GltS holoenzyme, while we confirmed that the isolated GltS  $\alpha$  subunit exhibits a strong glutaminase activity (not shown). From these data it appears that both 2-oxoglutarate and bound reduced ferredoxin are required to allow binding and/or hydrolysis of L-glutamine at the glutamine amidotransferase site of Fd-GltS. To gain further information on the factors that are necessary to determine activation of the glutamine amidotransferase site of Fd-GltS, we examined the effect of 6-diazo-5-oxo-L-norleucine (L-DON) on the reaction of Fd-GltS. L-DON is a well-known glutamine analogue that acts as a covalent irreversible inactivator of amidotransferases by forming a covalent addition product with the catalytically essential cysteine residue in the glutamine amidotransferase active subsite (35). L-DON is a potent inhibitor of Ab-GltS (36). At a concentration of 1 mM it fully inactivates the enzyme within the first minute of incubation at 25 °C. Control experiments were carried out during the course of the present work with Ab-GltS and its  $\alpha$  subunit using the procedures adopted to study the effect of L-DON on Fd-GltS. Such control experiments confirmed that under our experimental conditions L-DON irreversibly and fully inactivates both enzymes (not shown). As shown in Table 3, L-DON was found to decrease the extent of glutamine conversion into glutamate when it was present in the assay mixture. On the contrary, it had no effect on enzyme activity when it was removed from incubation mixtures prior to assay for conversion of L-[U-<sup>14</sup>C]glutamine into glutamate. These results show that, contrary to expectations, L-DON acts as a reversible inhibitor of Fd-GltS rather than as a covalent irreversible inactivator. Thus, Fd-GltS differs significantly from the Ab-GltS holoenzyme and GltS  $\alpha$  subunit, which are fully and rapidly inactivated upon incubation with L-DON. This compound seems to be unable to bind and form the expected covalent addition product with the catalytic Cys(1) residue in the amidotransferase site of Fd-GltS even when the preincubation is carried out in the presence of Fd, 2-OG, and dithionite.

## CONCLUSIONS

The recent optimization of a protocol that allows the obtainment of significant amounts of *Synechocystis* Fd-GltS together with the availability of the recombinant forms of *A. brasilense* GltS holoenzyme and of its  $\alpha$  subunit allowed us to carry out for the first time a comparison of some of the properties of the plant-type ferredoxin-dependent form of the enzyme with those of the bacterial NADPH-dependent GltS and of its isolated  $\alpha$  subunit.

The overall properties of Fd-GltS and of Ab-GltS  $\alpha$  subunit are similar, as expected from the similarity of their primary structures. For example, they display an overall similar reactivity with sulfite and similar binding interaction with 2-OG, and in all cases the FMN flavin cofactor does not stabilize semiquinone species, which must be formed during catalysis. This finding suggests that also their three-dimensional structures must not be dramatically different. Significant, although limited, differences in the environment of the FMN cofactor and of the [3Fe-4S] cluster of the enzyme forms are, however, expected to reflect the different redox properties of the enzyme cofactors, which make the midpoint potential values of the centers of Fd-GltS less negative than those of the corresponding centers in Ab-GltS. However, the distribution of the midpoint potential values of the cofactors in Fd-GltS is consistent with an electron pathway from reduced ferredoxin to FMN which involves the enzyme [3Fe-4S] cluster (Scheme 3) similar to that proposed for Ab-GltS (Scheme 1; 7) with one of the two reduced ferredoxin molecules functionally replacing the Ab-GltS [4Fe-4S] cluster involved in electron transfer from FAD to FMN (Scheme 1; 7).

Fd-GltS is more similar to the Ab-GltS holoenzyme than to GltS  $\alpha$  subunit with respect to the tight coupling between the activities occurring at the glutamine amidotransferase and the glutamate synthase sites (Schemes 1 and 3). This was not unexpected since only Fd-GltS and the Ab-GltS holoenzyme are the physiological enzyme forms. As in the case

of Ab-GltS (23), 2-OG or reducing equivalents alone are not sufficient to trigger glutamine hydrolysis (Table 2). In Fd-GltS even reduced Fd alone is not sufficient to activate such reaction (Table 2). The three-dimensional structure of Ab-GltS  $\alpha$  subunit showed how such enzyme species is in a conformation in which the GAT site is able to bind and hydrolyze L-glutamine but unable to transfer it efficiently through the ammonia tunnel, which appears in a closed conformation being obstructed by several amino acyl side chains (3). Inspection of Ab-GltS  $\alpha$  subunit structure (3) and comparison of the properties of the isolated  $\alpha$  subunit with those of the Ab-GltS  $\alpha\beta$  holoenzyme led to the proposal that in the holoenzyme the GAT site should be in a conformation still capable to bind L-Gln (as shown by the fact that L-DON is a potent inactivator of Ab-GltS; Table 3 and ref 36) but unable to hydrolyze it. Binding of 2-OG and reduction of the enzyme cofactors of the synthase site (Scheme 1) should induce a long-range conformational change in the GAT domain, which activates L-Gln hydrolysis and its transfer to the synthase site (steps b and c of Scheme 2). Polypeptide stretches joining the synthase and GAT sites and forming the walls of the ammonia tunnel should be involved in such activation process (3). The present experiments show that also in the case of Fd-GltS the activities of the enzyme catalytic GAT and synthase sites are tightly controlled through long-distance conformational changes. Interestingly, in Fd-GltS it has been possible to demonstrate that the enzyme controls steps involving L-glutamine binding, hydrolysis, and/or transfer of ammonia between the GAT and synthase sites. The presence of 2-OG and the redox state of the enzyme cofactors are not sufficient to activate L-glutamine utilization. Rather, it is clearly shown that binding of reduced Fd is necessary (but not sufficient) to induce the conformational changes required to activate the GAT site and to promote ammonia transfer to the synthase site. How the observed functional differences among the enzyme forms under study reflect well-defined structural differences will be revealed by the comparison of the three-dimensional structure of Fd-GltS with those of Ab-GltS and of its isolated  $\alpha$  subunit. The three-dimensional structure of Ab-GltS  $\alpha$  subunit has been solved (3), *Synechocystis* Fd-GltS has been crystallized, its three-dimensional structure is being determined, and the search of crystallization conditions of the Ab-GltS holoenzyme is in progress.

## ACKNOWLEDGMENT

Drs. Giuliana Zanetti and Alessandro Aliverti are thanked for helpful suggestions on ferredoxin purification and handling.

## REFERENCES

1. Vanoni, M. A., and Curti, B. (1999) Glutamate synthase: a complex iron-sulfur flavoprotein, *Cell. Mol. Life Sci.* 55, 617–638.
2. Ravasio, S., Curti, B., and Vanoni, M. A. (2001) Determination of the midpoint potential of the FAD and FMN flavin cofactors and of the 3Fe/4S cluster of glutamate synthase, *Biochemistry* 40, 5533–5541.
3. Binda, C., Bossi, R., Wakatsuki, S., Artz, S., Coda, A., Curti, B., Vanoni, M. A., and Mattevi, A. (2000) Cross-talk and ammonia channeling between active centres in the unexpected domain arrangement of glutamate synthase, *Structure* 8, 1299–1308.
4. Navarro, F., Martin-Figueroa, E., Candau, P., and Florencio, F. J. (2000) Ferredoxin-dependent iron-sulfur flavoprotein from the cyanobacterium *Synechocystis* sp. PCC 6803: expression and assembly in *Escherichia coli*, *Arch. Biochem. Biophys.* 379, 267–276.
5. Knaff, D. B., and Hirasawa, M. (1991) Ferredoxin-dependent chloroplast enzymes, *Biochim. Biophys. Acta* 1056, 93–125.
6. Stabile, H., Curti, B., and Vanoni, M. A. (2000) Functional properties of recombinant *Azospirillum brasilense* glutamate synthase, a complex iron-sulfur flavoprotein, *Eur. J. Biochem.* 267, 2720–2730.
7. Vanoni, M. A., Fischer, F., Ravasio, S., Verzotti, E., Edmondson, D. E., Hagen, W. R., Zanetti, G., and Curti, B. (1998) The recombinant  $\alpha$  subunit of glutamate synthase: spectroscopic and catalytic properties, *Biochemistry* 37, 1828–1838.
8. Morandi, P., Valzasina, B., Colombo, C., Curti, B., and Vanoni, M. A. (2000) Glutamate synthase: identification of the NADPH binding site by site-directed mutagenesis, *Biochemistry* 39, 727–735.
9. Schmitz, S., Navarro, F., Kutzki, C. K., Florencio, F. J., and Boehme, H. (1996) Glutamate 94 of [2Fe-2S] ferredoxins is important for efficient electron transfer in the 1:1 complex formed with ferredoxin-glutamate synthase (GltS) from *Synechocystis* sp. PCC 6803, *Biochim. Biophys. Acta* 1277, 135–140.
10. Schmitz, S., and Boehme, H. (1995) Amino acid residues involved in functional interaction of vegetative cell ferredoxin from the cyanobacterium *Anabaena* sp. PCC 7120 with ferredoxin:NADP reductase, nitrite reductase and nitrate reductase, *Biochim. Biophys. Acta* 1231, 335–341.
11. Piubelli, L., Aliverti, A., Bellintani, F., and Zanetti, G. (1995) Spinach Ferredoxin I: overproduction in *Escherichia coli* and purification, *Protein Expression Purif.* 6, 298–304.
12. Bradford, M. M. (1976) A rapid and sensitive method for the quantitation of microgram quantities of protein utilizing the principle of protein-dye binding, *Anal. Biochem.* 72, 248–254.
13. Vanoni, M. A., Negri, A., Zanetti, G., Ronchi, S., and Curti, B. (1990) Structural studies on the subunits of glutamate synthase from *Azospirillum brasilense*, *Biochim. Biophys. Acta* 1039, 374–377.
14. Laemmli, U.K. (1970) Cleavage of structural proteins during the assembly of the head of bacteriophage T4, *Nature* 227, 680–687.
15. Vanoni, M. A., Edmondson, D. E., Zanetti, G., and Curti, B. (1992) Characterization of the flavins and the iron-sulfur centers of glutamate synthase from *Azospirillum brasilense* by absorption, circular dichroism, and electron paramagnetic resonance spectroscopies, *Biochemistry* 31, 4613–4623.
16. Aliverti, A., Curti, B., and Vanoni, M. A. (1999) Identifying and quantitating FAD and FMN in simple and iron-sulfur-containing flavoproteins, in *Methods in Molecular Biology, Flavoprotein Protocols* (Chapman, S. K., and Reid, G. A., Eds.), Vol. 131, pp 9–23, Humana Press, Totowa, NJ.
17. *The Merck Index* (2001) 13th ed., Merck & Co., Whitehouse Station, NJ.
18. Segel, I. H. (1975) in *Enzyme kinetics*, Wiley & Sons, New York.
19. Bevington, P. H. (1969) in *Data Reduction and error analysis for the physical sciences*, McGraw-Hill, New York.
20. Williams, C. H., Arscott, L. D., Matthews, R. G., Thorpe, C., and Wilkinson, K. D. (1979) Methodology employed for anaerobic spectrophotometric titrations and for computer-assisted data analysis, *Methods Enzymol.* 62, 185–207.
21. Orr, G. A., and Blanchard, J. S. (1984) High-performance ion-exchange separation of oxidized and reduced nicotinamide adenine dinucleotides, *Anal. Biochem.* 142, 232–234.
22. Penefsky, H. S. (1977) Reversible binding of Pi by beef heart mitochondrial adenosine triphosphatase, *J. Biol. Chem.* 252, 2891–2899.
23. Vanoni, M. A., Edmondson, D. E., Rescigno, M., Zanetti, G., and Curti, B. (1991) Mechanistic studies on *Azospirillum brasilense* glutamate synthase, *Biochemistry* 30, 11478–11484.
24. Engel, P. C., and Dalziel, K. (1967) The equilibrium constants of the glutamate dehydrogenases systems, *Biochem. J.* 105, 691–695.
25. Massey, V., Mueller, F., Feldberg, R., Schuman, M., Sullivan, P. A., Howell, L. G., Mayhew, S., Matthews, R. G., and Foust, G. P. (1969) The reactivity of flavoproteins with sulfite. Possible relevance to the problem of oxygen reactivity, *J. Biol. Chem.* 244, 3999–4006.
26. Hirasawa, M., Robertson, D. E., Ameyibor, E., Johnson, M. K., and Knaff, D. B. (1992) Oxidation-reduction properties of the ferredoxin-linked glutamate synthase from spinach leaf, *Biochim. Biophys. Acta* 1100, 105–108.

27. Hirasawa, M., Hurley, J. K., Salamon, Z., Tollin, G., and Knaff, D. B. (1996) Oxidation–reduction and transient kinetic studies of spinach ferredoxin-dependent glutamate synthase, *Biochim. Biophys. Acta* 330, 209–215.
28. Hunt, J., Massey, V., Dunham, W. R., and Sands, R. H. (1993) Redox potential of milk xanthine dehydrogenase, *J. Biol. Chem.* 268, 18685–18691.
29. Mueller, F. (1991) Free flavins: syntheses, chemical and physical properties, in *Chemistry and Biochemistry of flavoenzymes* (Muller, F., Ed.) Vol. 1, pp 1–71, CRC Press, Boca Raton, FL.
30. Vanoni, M. A., Nuzzi, L., Rescigno, M., Zanetti, G., and Curti, B. (1991) The kinetic mechanism of the reactions catalyzed by the glutamate synthase from *Azospirillum brasilense*, *Eur. J. Biochem.* 202, 181–189.
31. Bottin, H., and Lagoutte, B. (1992) Ferredoxin and flavodoxin from the cyanobacterium *Synechocystis* sp PCC 6803, *Biochim. Biophys. Acta* 1101, 48–56.
32. Marques, S., Florencio, F. J., and Candau, P. (1992) Purification and characterization of the ferredoxin-glutamate synthase from the unicellular cyanobacterium *Synechococcus* sp. PCC 6301, *Eur. J. Biochem.* 206, 69–77.
33. Galvan, F. Marquez, A. J., and Vega, J. M. (1984) Purification and molecular properties of ferredoxin-glutamate synthase from *Chlamydomonas reinhardtii*, *Planta* 162, 180–187.
34. Hirasawa, M., and Tamura, G. (1984) Flavin and iron–sulfur containing ferredoxin-linked glutamate synthase from spinach leaves, *J. Biochem.* 95, 983–994.
35. Zalkin, H., and Smith, J. (1998) Enzymes utilizing glutamine as an amide donor, *Adv. Enzymol. Relat. Areas* 72, 87–144.
36. Vanoni, M. A., Accornero, P., Carrera, G., and Curti, B. (1994) The pH dependent behaviour of catalytic activities of *Azospirillum brasilense* glutamate synthase and iodoacetamide modification of the enzyme provide evidence for a catalytic Cys-His ion pair, *Arch. Biochem. Biophys.* 309, 222–230.
37. Pelanda, R., Vanoni, M. A., Perego, M., Piubelli, L., Galizzi, A., Curti, B., and Zanetti, G. (1993) Glutamate synthase genes of the diazotroph *Azospirillum brasilense*. Cloning, sequencing, and analysis of functional domains, *J. Biol. Chem.* 268, 3099–3106.

BI020083R